

## OPTIMIZED OVERALL DESIGN OF A ROBOTIC ARC WELDING CELL AND CALCULATION PROCEDURES FOR OPTIMAL SELECTION OF IR MOTORS

Constantin DUMITRAȘCU<sup>1,\*</sup>, Florin Adrian NICOLESCU<sup>2</sup>, Cozmin Adrian CRISTOIU<sup>3</sup>

<sup>1)</sup> As. Prof. PhD., Quality Engineering and Industrial Technologies Dept., Politehnica University of Bucharest, Romania

<sup>2)</sup> Professor PhD., Robots and Manufacturing Systems Dept., Politehnica University of Bucharest, Romania

<sup>3)</sup> Lecturer PhD., Robots and Manufacturing Systems Dept., Politehnica University of Bucharest, Romania

**Abstract:** Robotic arc welding represents one of the most important industrial applications. After handling applications, arc welding is the most common industrial application, totaling over 66,000 new robotic cell installations by 2020 [1]. For this reason, in the development of new robotic cells two approaches may be of interest at present: the use of a pre-designed robotic cell and the development of a customized robotic cell for arc welding. Discussion on this issue regarding the involved advantages and disadvantages of each approach and conclusions are presented in the first part of the paper. The second part of the paper deals with a specific computational algorithm developed for the optimal selection of the engine of industrial robots. The specific steps of the calculation procedure detailed in the paper can be used for a large number of models of industrial robots used for arc welding or other industrial application. The application of the calculus procedure is exemplified in the paper on the optimum selection of the driving motors for the last three NC axis of an ABB IRB 2400 articulated arm industrial robot, but still the algorithm can be extended to the optimal sizing and selection of all IR driving motors. The computational algorithm can also be used for other IR models that have a similar design of the final effect orientation subsystem. The algorithm was intensively tested for many industrial robot models, and the calculation results were validated for all IR analyzed models.

**Key words:** arc welding cell, optimum robotic cell design, industrial robots, calculus algorithm, optimum driving motor selection.

### 1. INTRODUCTION. ACTUAL DEVELOPMENT STATUS OF ROBOTIC ARC WELDING CELLS

Robotic arc welding represents one of the most important industrial applications. Following the handling applications, arc welding represents the most common industrial application summing a total of over 66 000 new robotic cells installation in 2020 year (Fig. 1) [1].

In optimizing overall robotic cell design, different design principles are necessary to be considered for optimizing each type of arc welding cell / system. However, the most important issue regarding the optimizing overall robotic cell design is related to the arc welded part size. Furthermore, depending on the dimensions of the welded parts the robotic arc welding cell may be considered specific design features for:

- robotic arc welding small size parts, (so called *small scale robotic cells*);
- robotic arc welding medium size parts, (or so called *medium scale robotic cells/ systems*);
- robotic arc welding large / very large size parts, (or so called *large scale robotic cells/ systems*) [2].

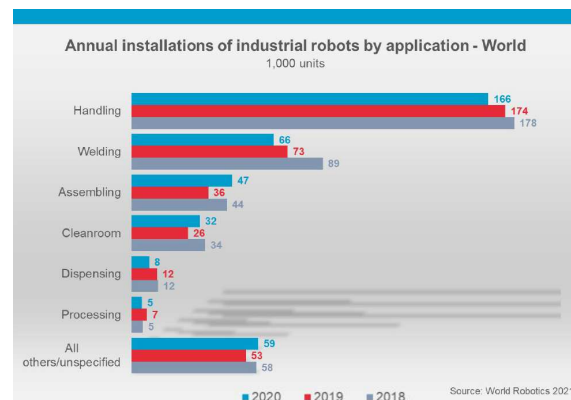


Fig. 1. Annual installation of industrial robots by application – World Robotics 2021 [1].

Considering this issue, first part of the present paper discusses only the case of small-scale robotic cells optimum design, in regard of pros and contras for selecting / designing and implementing a *pre-engineered arc welding robotic cell* or a *custom designed arc welding robotic cell*, respectively. Conclusions regarding the appropriate approach for specific industrial users are also presented.

The second part of the paper continues the optimization approach on the specific IR optimum design level by detailing a calculus procedure for IR driving

\* Corresponding author: Institution address,  
 Tel.: +40.744.923.533.

E-mail addresses: [afnicolescu@yahoo.com](mailto:afnicolescu@yahoo.com) (A. Nicolescu),  
[costishor40@yahoo.com](mailto:costishor40@yahoo.com) (C. Dumitrascu).

motors optimum selection. Constructive and functional specifications for a selected IR model, overall gravitational and inertial load distribution on IR and their reducing on the load reducing centers level for each IR NC axis, evaluation of the inertial loads generated by mechanical components included IR NC axis, applying the iterative optimum sizing and selection algorithm for IR driving motors, (including the kinematic, static, dynamic and the performance parameters criteria) as well as Final results of iterative calculations and conclusions about optimum selected driving motors are included. Final conclusions regarding the technical and scientific contributions are also presented [3].

## 2. PRE-ENGINEERED VERSUS CUSTOM DESIGNED ARC WELDING CELLS

### 2.1. Pre-engineered robotic arc welding cells

Pre-engineered robotic cells are standardized units that are already fully integrated. The most common pre-engineered work cells are designed for arc welding applications. Manufacturers as ABB, Motoman, KUKA, (Fig. 2) [4], Panasonic, Kawasaki and Fanuc carry their own lines of standardized weld cells including 1, 2 or even 3 robots and different types of part positioners.

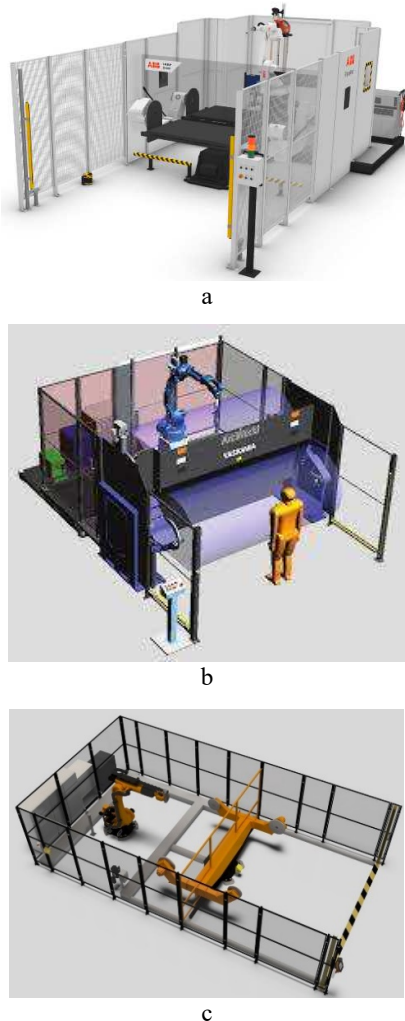


Fig. 2. Pre-engineered robotic cells: a – ABB; b – Motoman; c – Kuka, arc welding cells.

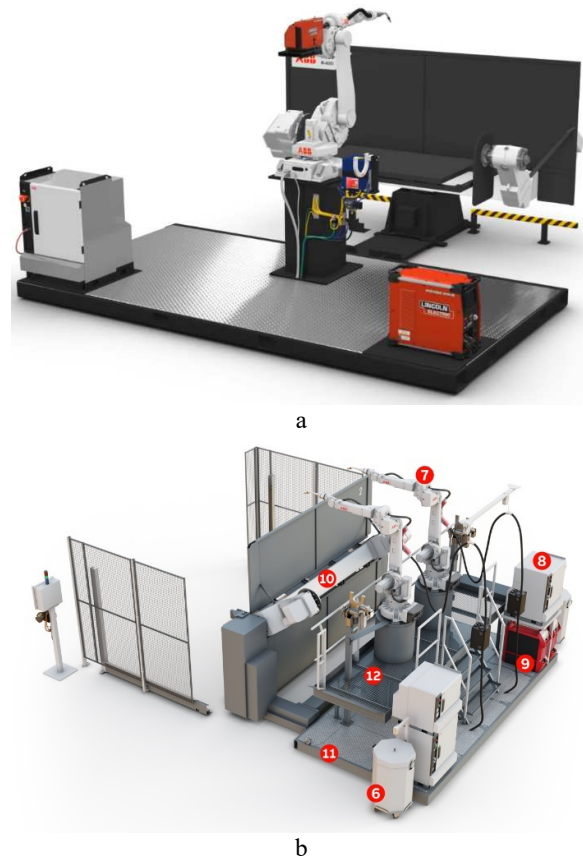


Fig. 3. Basic modular components of ABB pre-engineered robotic cells: a – single IR cell; b – dual IR cell.

A pre-engineered robotic cell consists of a base-frame table, a robot, torch, wire feeder system and welding dressing, a welding power source, and a safety enclosure. The basic frame carries all components such as robot(s) with control cabinet, part positioning system, torch management system, power source and safety devices, as well as has set all power connections [5]. The entire production cell is built on a self-supporting base frame and forms a transport and stacking unit. It is typically shipped as a single, self-contained unit, pre-assembled [6]. Basically, being connected to the power source, the units are ready to weld after the connection of assistance gas. Safety enclosures and fume extractor installation can be finally added [2].

Generally, the system concept is based on the 2-station principle (Fig. 3,b) [7]. While the robot is working in the first station, the operator can remove the finished welded component in parallel in the other station and then retrofit it. After loading, the operator activates the start button. If the component is finished by the robot on the corresponding working side, the change of the station is carried out automatically and the cycle begins anew. The processing time of the robot can thus be used optimally for a specific range of products targeted to be processed [6].

However, a pre-engineered robotic welding cell is designed for welding specific parts in a certain size range. Pre-engineered cells offer benefits for easy and fast installation and a lower first cost, but they do have their limitations regarding the type and size of parts that can be welded. Part size and welds complexity are often

the key determining factor when choosing a pre-engineered robotic weld cell [8].

Pre-engineered work cells tend to be application specific and provide already proven solutions for that kind of application. These cells are best suited for small sized parts and medium to high-volume productions. Also, parts that are regular in shape and do not require much manipulation during welding are candidates for standardized systems [8].

The biggest advantage of pre-engineered cells over custom ones is their short delivery time. Work cells arrive with little wait time and ready for operation, allowing users to start works quickly. In addition, they are much more cost-effective with all equipment pre-installed and sold as a single package. In case of ordering to same supplier the fixture system for some pre-set parts, additional time and money are not needed for engineering [8].

Disadvantages of pre-designed work cells include the inability to handle medium to large workpieces, uneven manufacturing processes, or complex applications. Standardized cells are not specific to a manufacturer. Some adjustments may be needed to their production process in order to start operation of the work cell, including fixturing system, design and implementing [8].

## 2.2. Custom designed robotic arc welding cells

Custom work cells are designed and engineered toward a customer specifications. Manufacturers usually turn to custom designs when their manufacturing process is more complex, parts are too large, workpieces require repositioning multiple times, or for when their application does not fall within pre-engineered cell designs. With customized cells, users get to select the robot, equipment, and safety devices, which can be beneficial [8].

A manufacturer can choose the industrial robot they like the most along with all additional equipment (Fig. 4). However, sometime, if not experienced in robotics and work cell design, this can be a drawback as there are numerous options to select from and more time consuming. For instance, a manufacturer designing an assembly work cell could find the FANUC M-20iA, the Motoman MH24, or the ABB IRB 2600 to all be an ideal fit, facing some difficulties in the sub-systems selection process [8].

That is why in order to achieve successfully the cell design the manufacturer need usually to address to an integrator with specific experience in this field of activity. Thus, when installing either type of robotic weld

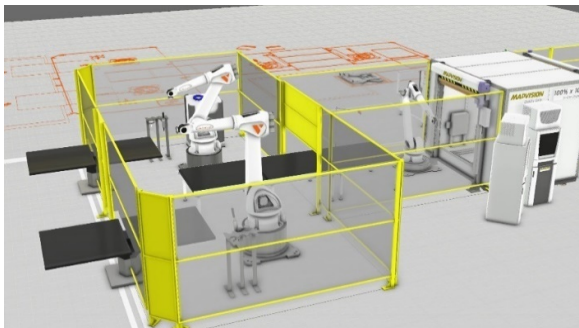


Fig. 4. Sample of custom-made robotic arc welding cells.

cell, the system integrator should be involved in planning and testing to ensure cell layout is optimized for the application [8].

If there is not a pre-engineered robotic weld cell available to perfectly fit the part welding, then a custom cell is the better option [8].

First issue to consider is that custom cells have a higher initial cost and typically a longer lead time for design and installation, but the upside is they can be customized to meet the specific needs: a welding system that does exactly what is needed without extras that are not necessary / cannot be use [2].

Basically, custom work cells are significantly more expensive than pre-engineered ones, since all equipment is not sold as a bundle and engineering is needed for the design and installation. Delivery time is much longer, since the cell will need to be designed and built from scratch. There is also necessary to consider risks of the application process not being effective from the first approach / design of the work cell that may take many adjustments to correct fit. On the other hand, in the end the system is fully customized to the user, so changes to a manufacturing process should not be needed. Many custom systems can also design from the beginning as be able for further expanded or integrate with other workstations or processes as needs change, so custom cells are also capable of handling any irregularities in part shape or size [8].

Custom equipment is generally designed and installed by an automation integrator. Because no two manufacturers have the same process, custom systems let tailor the system to what is most important in each situation in direct comprehensive discussions with the manufacturer [9].

As result, to make a high-mix, low-volume operation more efficient, an integrator may bring together single components to coordinate material handling, communications between devices, fixturing, and the actual welding robot and equipment. Beside of this it is also usually responsible for designing sets of different fixtures for full current range of part manufacturing [9].

## 3. OPTIMUM OVERALL DESIGN OF A ROBOTIC ARC WELDING CELL

### 3.1. The reference model for starting up the study of robotic arc welding cell optimum design

The reference model in starting the study activities of the optimization possibilities is a compact robotic electric arc welding cell (from ABB pre-engineered cell series), that integrates an industrial robot with articulated arm architecture and a peripheral positioning system with two workstations (Fig. 5,a and b) [4].

The cell is served by a human operator with the role of loading semi-finished products / unloading welded parts in / from the peripheral positioning system.

The individual parts used in final product manufacturing as well as the final product are stored near the welding cell in special dedicated containers.

Manual fixture set is used for part preliminary fixing in a specific device mounted on each positioner workstations.

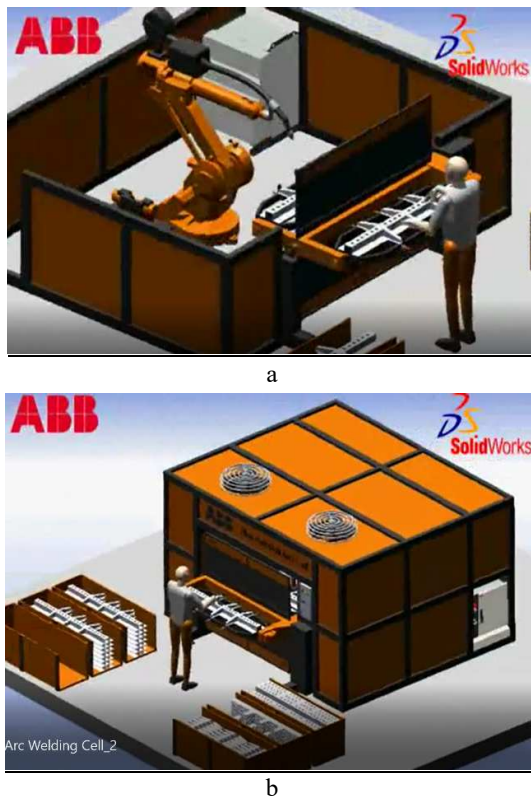


Fig. 5. The reference model for the robotic arc welding cell [4].

Main issues to be improved for the selected reference model of arc welding robotic cell design and operation are considering:

- the legal limits existing in part weight to be manipulated by human operator along 8 hours continuous working shift, (for human operator protection against professional diseases) specifying a maximum handled part payload, up to 20–25 kg payload (for men), and, up to 8–9 kg payload (for women);
- the decreased level of cell productivity for complex welded products. Row material parts to be welded are stored outside of the serviced area, thus the human operator needs to repeatedly pick-up and transport each row material part, insert it in the fixturing device and fix it by manually operated clamping system;
- the important size of the storage area for different row material parts and final products, in special dedicated containers (usually this area varies between (30–50)% up to 100% of the arc welding robotic cell itself), thus, an important amount of production space is stuck of these containers;
- inside the arc welding robot operation area, the welding electrode storage system has limited capacity of storage and is not conveniently disposed for its rapidly replacing when empty of wire electrode. Starting up from the existing cell model, an improved design of the arc welding robotic cell has been developed (Fig. 6, a, b, and c) [10].
- replacing the human operator that serve the cell by an industrial robot for loading semi-finished products / unloading welded parts in / from the peripheral positioning system;

- replacing the manual operated clamping devices of the part fixturing system by pneumatic driven devices;
- eliminating the row material and finished parts storage containers and replacing them by a pallet conveyor transporting modular pallets able to be configured for transporting both, kits of parts to be welded (on income stage), as well as the final products (on outcome stage);
- relocating the wire electrode storage system outside of the arc welding robot operation area (for an improved serviceability), adding a complementary wire feeding system (that may be used in a tandem push-pull wire operation procedure) and preparing a wire electrode large storage capacity system, for replacing the wire electrode low storage capacity included in the reference robotic arc welding cell.

Based on the above-mentioned improvements the arc welding robotic cell increase in operational level due to:

- reducing of the necessary space for cell layout, by eliminating the storage area. For stand-alone arc

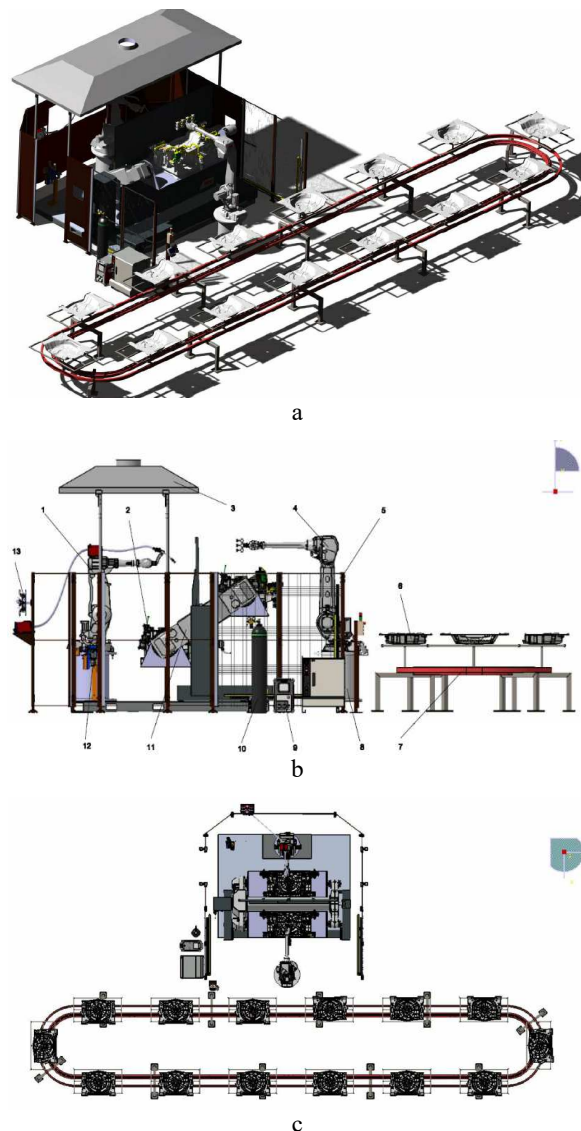


Fig. 6. Improved design of the arc welding robotic cell: a – perspective view; b – lateral view; c – top view [10].

welding cells, the pallet conveyor may be set as an closed loop model. At the same time, for serving multiple interconnected cells, it may be replaced by an *in-line conveyor*, (as is the case of usual manufacturing facilities) and their interconnection with an AS-RS system. Thus, the AS-RS system is usually used for central storage of pallets with row material parts kits and joined with the in-line conveyor it may *just in time* supply the right set of row material parts to the appropriate robotic cell / recover and store all welded products.

- however, for adapting the loading / unloading IR to a new set of row parts / new welded products manipulation a tool storage stand, for different robotic end-effectors and an automated tool changing system need to complete the actual robotic cell design. In this approach, the pallet conveyor may be also used to transport the replacement fixturing devices through each robotic cell, and the automated exchanging of the fixturing device may be also performed by the same loading / unloading IR equipped with the automated tool changing system. (Complementary auxiliary device for uncoupling and coupling the old / new fixturing system on the peripheral equipment need also be implemented in such cases);
- increasing the overall robotic cell productivity by reducing the auxiliary operational time necessary for row materials part fixing / final product releasing due to pneumatic automation of the clamping devices included in the fixturing system;
- increasing the overall robotic cell productivity by reducing the auxiliary operational time necessary for periodically replacing low storage volume of electrode wire system, due to its outside location as well as preparing the arc welding cell for implementing a large storage wire electrode system (actually included in any new design of arc welding robotic cell);
- using the VirtualArc software [11] for setting the appropriate arc welding equipment and process technological parameters by using the ABB special dedicated PC tool for off-line arc welding prediction and robotic MIG/MAG arc welding tuning (Fig. 7);
- using the RoboDK software package for off-line programming and simulation of arc welding robotic cell, in order to define and finally checking of tool

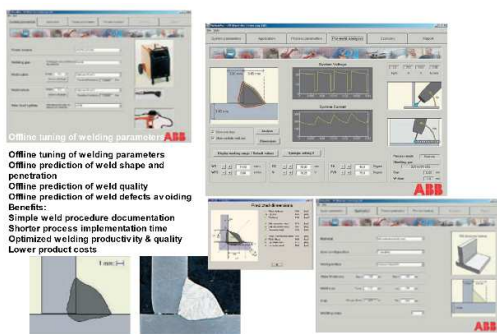


Fig. 7. ABB PC tool for off-line arc welding prediction and robotic MIG/MAG arc welding tuning.

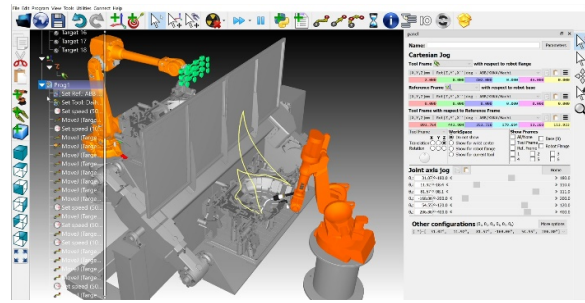


Fig. 8. RoboDK software package for off-line programming and simulation of arc welding robotic cell.

path through via points, arc welding trajectories and tool orienting along their generation by tool TCP, as well as collision avoidance of the tool with the fixturing system and complementary devices (Fig. 8) [12].

### 3.2. Conclusions regarding the appropriate approach for specific industrial users

The complete structure of a arc welding robotic cell need to include [2, 3]:

- industrial robot(s) – usually articulated arm;
- supporting structure:
  - pedestal / base (for raising the RI base);
  - 1/2/3/4 NC axis for IR work-space extension (by IR base rotation / translation);
- IR technological equipment:
  - the specialized effector(s) – arc welding torch type;
  - the automatic wire feeding system – consumable electrode advancement (calibrated wire);
  - the electrode consumable storage system attached to RI (if drum type storage device is used);
  - IR arc welding dressing (the system of hoses and cables allowing the management of the utilities from the power source / electrode storage system / assistance gas supplying system / torch cooling system to IR effector);
- technological equipment for electric arc welding:
  - power source for welding (minimum MIG + MAG, optional including facilities for TIG, WIG);
  - assistance gas supplying system (inert / active gas for non-metallic / metallic parts arc welding);
  - forced cooling system or the welding torch;
  - welding torch management system (with wire cutting, torch nose cleaning and torch calibration functionalities);
  - large size storage system for consumable electrode (if using an increased capacity of electrode storage system);
  - arc welding opaque enclosure of the robotic welding area, (for operator view protection);
  - fume extractor and air filtering system;
- peripheral robotic system for positioning / additional orientation of the welded parts;
- control panel for the human operator interfacing (stop in case of failure + confirmation of closing actions in dedicated work cell space for human operators);
- safety systems – sensors for safety operation of the human operator protection and conditioning of robotic cell operation with human operator

interventions (light barriers, retractable curtains, carpets with pressure sensors, laser scanner, etc.);

- enclosure panels for delimiting the overall arc welding work cell operational space;
- robot controller (IR control and programming equipment);
- process controller (control equipment for setting up process parameters related to electric arc welding process and cell operation).

However, when setting up a specific investment for a robotic arc welding cell, it will be necessary to consider that all of these included sub-systems / equipment, usually lead to reach a 4 time up to 10 times greater price of the overall arc welding robotic cell system versus the price of the IR itself.

#### 4. CALCULATION PROCEDURE FOR OPTIMAL SELECTION OF IR DRIVING ENGINES

Calculus procedure for IR driving motors optimum selection includes following steps:

- Identifying the reference IR model, its constructive and functional specifications, the internal mechanical structure of 3rd, 4th and 5th IR NC axes and the specific location of load reducing centers for each IR NC axis.
- Evaluation of IR partial assembly volumes and masses as well as identifying their mass center location.
- Evaluation of overall gravitational and inertial load distribution on IR. Reducing of the overall load distribution, first in the load reducing centers for each IR NC axis and second on driving motor shaft level.
- Evaluation of the inertial loads generated by mechanical components included in 3rd, 4th and 5th IR NC axes, and their reduction on driving motor shaft level.
- Applying the optimum sizing and selection criteria for IR driving motors. The kinematic criteria, the static criteria, the dynamic criteria, and the performance parameters criteria applying.
- Final results of iterative calculations and conclusions about optimum selected driving motors.

However, the calculus algorithm may be used both: for designing a new IR, or as well, for optimum selecting an existing version of IR based on identifying the specific operation conditions for its driving motors.

##### 4.1. Identifying the reference IR model

As specified from the pre-engineered robotic arc welding cell data sheet, the reference IR model, is an IRB 2400. This IR model may be supplied in two versions: for a maximum payload of 16 kg or for a maximum payload of 10 kg, the difference between the two versions being the size of the included IR driving motors for end-effector orienting. However, the internal mechanical structure of IR 4th, 5th and 6th NC axes is the same for both variants. That is why the algorithm will be applied only for IR 4th, 5th and 6th NC axis motor operation conditions identifying and their optimum selection.

The reference IR model is presented in Fig. 9 [13]. Constructive and functional specifications are presented



Fig. 9. The reference ABB IRB 2400 IR model [13].

in Table 1 and Fig. 10. The internal mechanical structure of 3rd, 4th and 5th IR NC axis and the specific location of load reducing centers for 4th, 5th and 6th IR NC axes are presented in Fig. 11.

- maximum payload: 10 kg / 16 kg;
- NC axis number: 6;
- IR Controller type: IRC 5;
- maximum reach: 1.564 m;
- position repeatability: 0.03 mm;
- robot weight: 380 kg [13].

Table 1

Working space and maximum speeds of IRB 2400 IR [13]

Axis Number	Working range	Speed
Axis 1	$\pm 180^\circ$	150 °/s
Axis 2	$-100^\circ / +110^\circ$	150 °/s
Axis 3	$-60^\circ / +65^\circ$	150 °/s
Axis 4	$\pm 200^\circ$	360 °/s
Axis 5	$\pm 120^\circ$	360 °/s
Axis 6	$\pm 400^\circ$	450 °/s

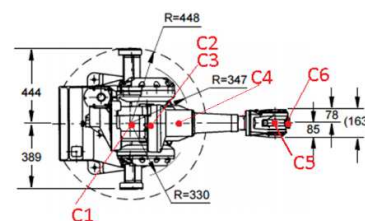
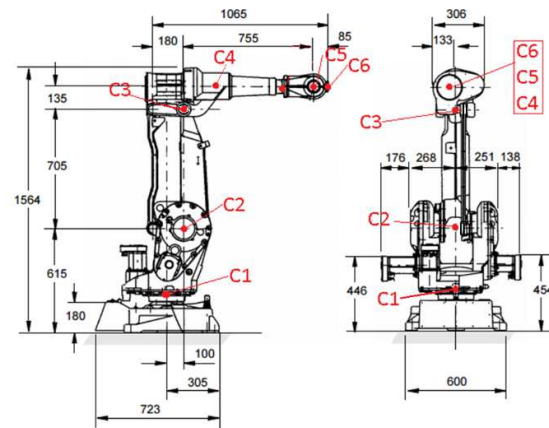
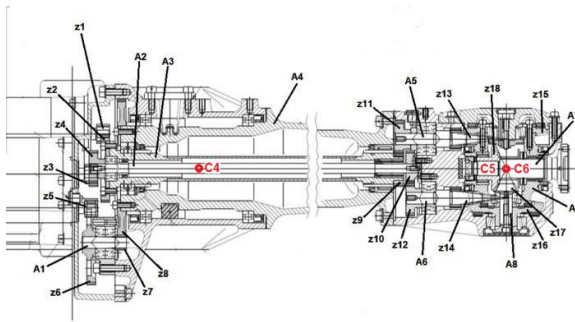


Fig. 10. Constructive-functional specifications of ABB IRB 2400 IR and overall calculus of center locations (C1...C6) [3, 13].



**Fig. 11.** The internal mechanical structure of 3rd, 4th and 5th IR NC axis and the specific location of load reducing centers for 4th, 5th and 6th IR NC axes [3, 13].

**4.2. Evaluation of IR partial assembly volumes and masses, and identifying their mass center location**

For identifying the partial assembly volumes, mass and mass center location a specific procedure need to be follow up:

- first, a carefully study of IR generally assembly is made in order to correctly identify its partial assemblies;
- second the CAD 3D file of the overall IR is loaded in Catia 3D solid modeling software (Fig. 12);
- third, necessary components for each partial assembly isolation are successively selected. For the group of components already selected as included in a partial assembly, total volume and mass center coordinates of each partial assembly are identified, by appealing the Measuring Inertia option (Figs. 13–20).

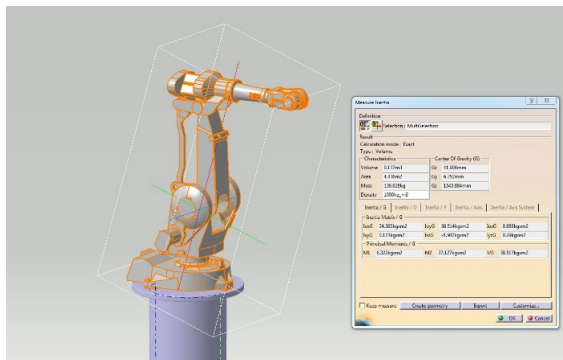


**Fig. 12.** Identifying the total IR volume and mass center coordinates [3, 10].

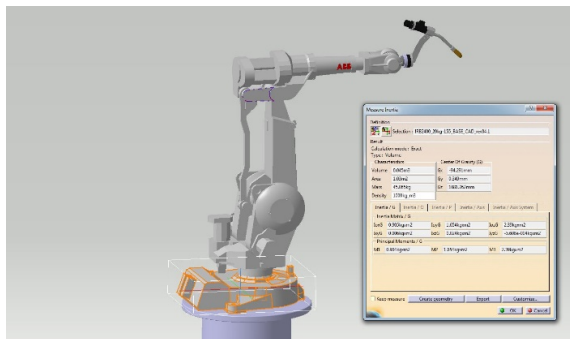


**Fig. 13.** Identifying the partial volume and mass center coordinates of IR partial assembly corresponding to the fixed part of IR joint 1 [3, 10].



**Fig. 14.** Identifying the partial volume and mass center coordinates of IR partial assembly corresponding to the mobile part of IR joint 1 and fixed part of joint 2 [3, 10].



**Fig. 15.** Identifying the partial volume and mass center coordinates of IR partial assembly corresponding to the mobile part of IR joint 2 and fixed part of joint 3 [3, 10].

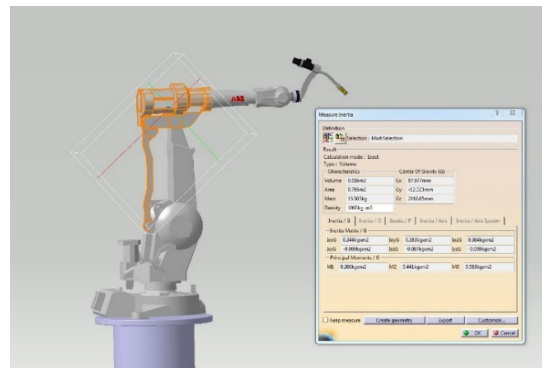


**Fig. 16.** Identifying the partial volume and mass center coordinates of IR partial assembly corresponding to the mobile part of IR joint 3 and fixed part of joint 4 [3, 10].



**Fig. 17.** Identifying the partial volume and mass center coordinates of IR partial assembly corresponding to the mobile part of IR joint 4 and fixed part of joint 5 [3, 10].

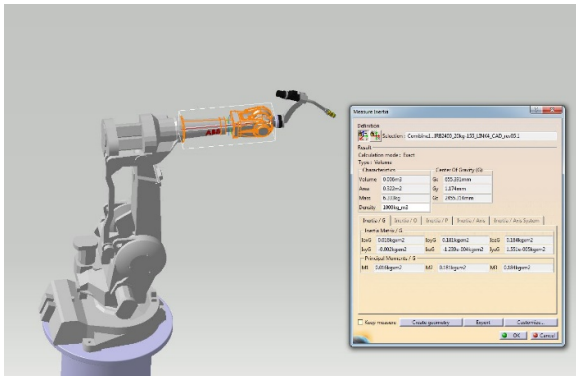


Fig. 18. Identifying the partial volume and mass center coordinates of IR partial assembly corresponding to the mobile part of IR joint 5 and fixed part of joint 6 [3, 10].

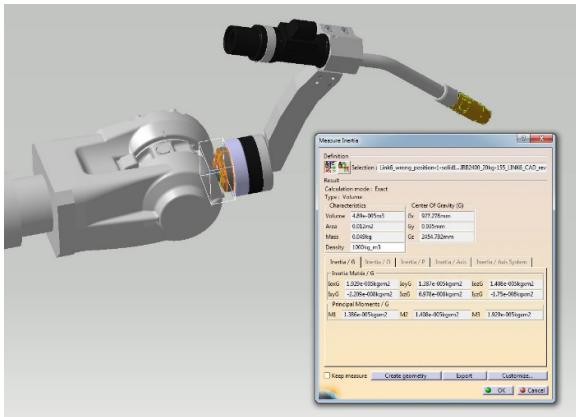


Fig. 19. Identifying the partial volume and mass center coordinates of IR partial assembly corresponding to the mobile part of IR joint 6 [3, 10].

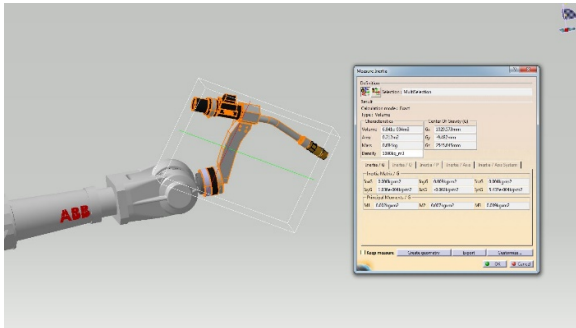


Fig. 20. Identifying the partial volume, mass and mass center coordinates of IR end-effector [3, 10].

- fourth, the following procedure is applied for identifying the partial mass of each above-mentioned IR partial assembly. For this purpose, the total mass of the IR is distributed by the corresponding percentage of each partial volume previously evaluated in Catia for each partial assembly, by applying following equations:

$$V_t = V_1 + V_2 + V_3 + V_4 + V_5 + V_6, \quad (1)$$

$$V_t = 0.045 + 0.052 + 0.016 + 0.016 + 0.006 + 0.000049 = 0.135 \text{ m}^3 \quad (2)$$

$$V_{P1} = \frac{V_1}{V_t} \cdot 100 = \frac{0.045}{0.135} \cdot 100 = 33.33\%, \quad (3)$$

$$V_{P2} = \frac{V_2}{V_t} \cdot 100 = \frac{0.052}{0.135} \cdot 100 = 38.52\%, \quad (4)$$

$$V_{P3} = \frac{V_3}{V_t} \cdot 100 = \frac{0.016}{0.135} \cdot 100 = 11.85\%, \quad (5)$$

$$V_{P4} = \frac{V_4}{V_t} \cdot 100 = \frac{0.016}{0.135} \cdot 100 = 11.85\%, \quad (6)$$

$$V_{P5} = \frac{V_5}{V_t} \cdot 100 = \frac{0.006}{0.135} \cdot 100 = 4.44\%, \quad (7)$$

$$V_{P6} = \frac{V_6}{V_t} \cdot 100 = \frac{0.000049}{0.135} \cdot 100 = 0.036\%, \quad (8)$$

and considering the total mass of ABB IRB 2600 IR as being 380 kg, successively may be determined:

$$m_t = m_1 + m_2 + m_3 + m_4 + m_5 + m_6 = 380 \text{ kg}, \quad (9)$$

$$m_1 = m_t \cdot V_{P1} = \frac{380 \cdot 33.33}{100} = 126.65 \text{ kg}, \quad (10)$$

$$m_2 = m_t \cdot V_{P2} = \frac{380 \cdot 38.52}{100} = 146.38 \text{ kg}, \quad (11)$$

$$m_3 = m_t \cdot V_{P3} = \frac{380 \cdot 11.85}{100} = 45.03 \text{ kg}, \quad (12)$$

$$m_4 = m_t \cdot V_{P4} = \frac{380 \cdot 11.85}{100} = 45.03 \text{ kg}, \quad (13)$$

$$m_5 = m_t \cdot V_{P5} = \frac{380 \cdot 4.44}{100} = 16.87 \text{ kg}, \quad (14)$$

$$m_{G17} = m_t \cdot V_{P6} = \frac{380 \cdot 0.036}{100} = 0.13 \text{ kg}, \quad (15)$$

$$m_t = 126.65 + 146.38 + 45.03 + 45.03 + 16.87 + 0.13 = 380 \text{ kg}. \quad (16)$$

Independently from above performed calculus procedure, after its 3D complete modelling, the total mass and specific mass center location of the IR end-effector is determined by using the same Catia – Measure Inertia option.

$$m_{ef} = m_B = 4.524 \text{ kg}. \quad (17)$$

#### 4.3. Evaluation of overall gravitational and inertial load distribution on IR. Reducing of the overall load distribution, in the load reducing centers for each IR NC axis and on driving motor shaft level.

In order for starting the evaluation of the overall gravitational and inertial load distribution on IR as well as the reducing of the overall load distribution, in the load reducing centers for each IR NC axis, a full set of geometric parameters (Table 2) need to be determined, part of them being directly identified from the constructive – functional specifications presented in Fig. 10 –and part of them from simply geometric consideration.

The specific values of these geometric parameters are presented in Table 2 [10]:

Furthermore, for evaluation of overall gravitational and inertial load distribution on IR a basic calculus

Table 2  
Geometric parameters for load distribution evaluation [10]

LC1	LC2	LC3	LC4	LC5	LC6
[mm]	[mm]	[mm]	[mm]	[mm]	[mm]
205	410	705	180	755	85

LG1	LG2	LG3	LG4	LG5	LG6	LG7	LG8	LG9
[mm]	[mm]	[mm]	[mm]	[mm]	[mm]	[mm]	[mm]	[mm]
82	445	491.5	135	575	40	85	135	170

schema is elaborated (Fig. 21), by considering the most unfavorable IR configuration along its working cycle, as well as previously identified values for the specific mass values and mass center location coordinates of all IR partial assemblies, and respectively the specific locations of the calculus centers for all IR NC axes.

Starting up from this basic calculation schema, step by step, there are successively identified, evaluated and represented (on particular loading schemas) the overall gravitational load distribution (Fig. 22), and respectively sets of inertial loads corresponding to each possibility of motion generated by IR major joints from the positioning system. For each IR active joint, as showed for the 1st joint in Fig. 23, for 2nd joint in Fig. 24 and for 3rd joint in Fig. 25, specific values of rotational motion speeds ( $\omega_1$ ,  $\omega_2$  and  $\omega_3$ ), as well as specific values and direction of the kinematic radius have been considered.

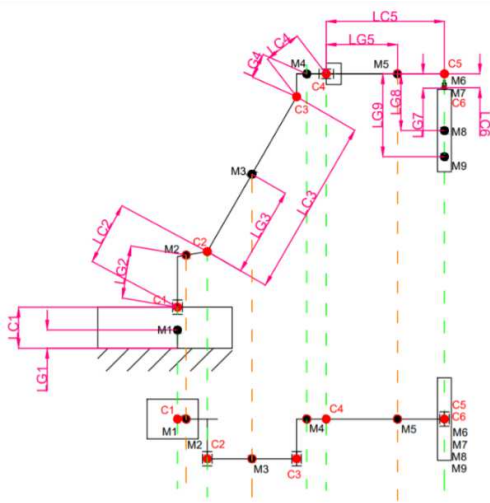


Fig. 21. Basic calculus schema for load distribution evaluation [3, 10].

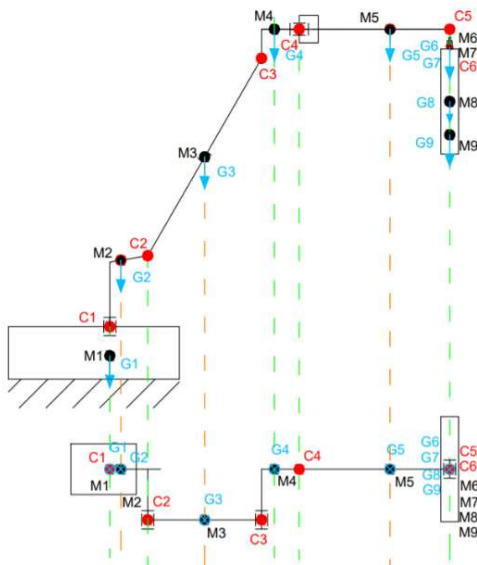


Fig. 22. Specific calculation schema for evaluation of IR gravitational loads overall distribution [3, 10].

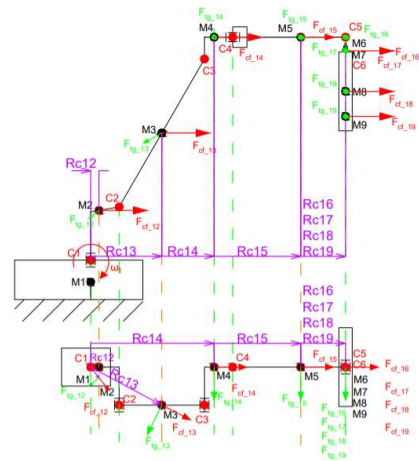


Fig. 23. Specific calculation schema for evaluation overall distribution of IR inertial loads generated by joint 1 rotation [3, 10].

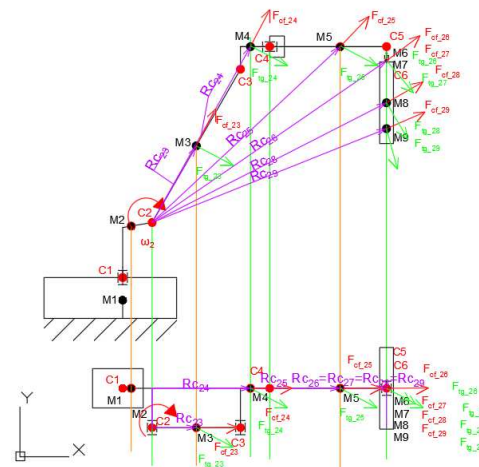


Fig. 24. Specific calculation schema for evaluation overall distribution of IR inertial loads generated by joint 2 rotation [3, 10].

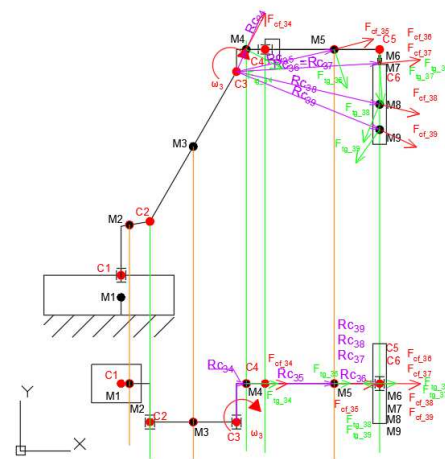


Fig. 25. Specific calculation schema for evaluation overall distribution of IR inertial loads generated by joint 3 rotation [3, 10].

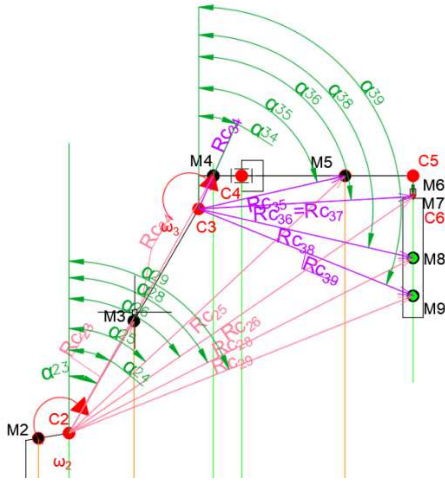


Fig. 26. Calculus schema for superposing gravitational and inertial load distribution effect and their reduction in the calculus centers C6, C5 and C4 [3, 10].

Furthermore, for evaluation of the overall effect of all gravitational and inertial loads, the superposing effect is applied, and reduced loads calculation in each calculus center is performed as Fig. 26 shows and below equation summarize for the case of calculus of center C6.

As result of these calculation, a complete set of three reduced forces and three reduced torques may be evaluated as below equations are showing for C6 calculus center case:

$$F_x^{RED} = \sum_{i=7}^9 F_i^x = 60.02 \text{ N}, \quad (18)$$

$$F_y^{RED} = \sum_{i=7}^9 F_i^y = 207.05 \text{ N}, \quad (19)$$

$$F_z^{RED} = \sum_{i=7}^9 F_i^z = -180.88 \text{ N}, \quad (20)$$

$$M_x^{RED} = F_7^y \cdot (LG_7 - LC_6) + F_8^y \cdot (LG_8 - LC_6) + F_9^y \cdot (LG_9 - LC_6) = 52.667 \cdot 10^{-3} \text{ Nm}, \quad (21)$$

$$M_y^{RED} = F_7^x \cdot (LG_7 - LC_6) + F_8^x \cdot (LG_8 - LC_6) + F_9^x \cdot (LG_9 - LC_6) = 15.623 \cdot 10^{-3} \text{ Nm}, \quad (22)$$

$$M_z^{RED} = 0. \quad (23)$$

The corresponding reduced forces and torques are used: first, to evaluate the total static torque and the first part of the dynamic torque applied to the IR axis 6 driving motor (that will be further presented) and second to determine the equivalent loads applied to the bearing system of the axis 6 mobile element, as shown following equations:

$$F_A = F_z^{RED} = -180.88 \text{ N}, \quad (24)$$

$$F_R = \sqrt{F_x^{RED^2} + F_y^{RED^2}} = 215.57 \text{ N}, \quad (25)$$

$$M^{RED} = \sqrt{M_x^{RED^2} + M_y^{RED^2}} = 54.93 \cdot 10^{-3} \text{ Nm}. \quad (26)$$

However, for the evaluation of the total dynamic torque applied to the IR axis 6 driving motor, supplementary to the first part of the dynamic torque (already above calculated), a complementary second torsional torque, (generated by the reflected inertia of all included mechanical components included in axis 6) reduced on the driving motor shaft need to be evaluated too, as follows:

$$M_{z_{joint\ 6}} = (J_{effector} + J_{flange}) \cdot \varepsilon_{joint\ 6} =$$

$$(0.006 + 0.0000193) \cdot \frac{7800}{1000} \cdot 17.44 = 0.819 \text{ Nm}, \quad (27)$$

$$\omega_{joint\ 6} = 450^\circ/s = 8.72 \text{ rad/s}, \quad (28)$$

$$\varepsilon_{joint\ 6} = \frac{\omega_{joint\ 6}}{t_{fr}} = \frac{8.72}{0.5} = 17.44 \text{ rad/s}^2, \quad (29)$$

$$\varepsilon_{joint\ 6} = \varepsilon_{EM\ shaft} \cdot \frac{z_7}{z_8} \cdot \frac{z_5}{z_6} \cdot \frac{z_3}{z_4} \cdot \frac{z_1}{z_2} = \varepsilon_{EM\ shaft} \cdot \frac{1}{2} \cdot \frac{1}{1} \cdot \frac{1}{5} \cdot \frac{1}{2}, \quad (30)$$

$$\varepsilon_{EM\ shaft} = \varepsilon_{joint\ 6} \cdot 2 \cdot 5 \cdot 1 \cdot 2 = 17.44 \cdot 20 = 348.8 \frac{\text{rad}}{\text{s}^2} = \frac{\omega_{maxnec\ EM}}{t_{brake}}, \Rightarrow \quad (31)$$

$$\omega_{maxnec\ EM} = 174.4 \frac{\text{rad}}{\text{s}} = 1665.39 \text{ rpm}, \quad (32)$$

where the kinematic transfer ratios of the included mechanical components (Fig. 10) have been considered:

$$\frac{z_{17}}{z_{18}} = \frac{1}{2}; \frac{z_{14}}{z_{16}} = \frac{1}{5}; \frac{z_{10}}{z_{12}} = \frac{1}{1}; \frac{z_8}{z_4} = \frac{1}{2}, \quad (33)$$

$$J_{RED\ joint\ 6} = J_{flange} + J_{effector} = 0.819 \text{ kg m}^2, \quad (34)$$

considering  $\rho = 7860 \text{ kg/m}^3$  for all steel parts.

Next, in order the evaluated specific inertia of each included mechanical component following equations were used:

$$I_{A7} = \frac{\rho \cdot \pi \cdot D_{m7}^4 \cdot h_7}{32} = 196.85 \cdot 10^{-6} \text{ kg m}^2 \quad (35)$$

$$I_{z_{18}} = \frac{\rho \cdot \pi \cdot R^2 \cdot B_{18} \cdot (D_{out\ med\ 18}^4 - D_{inn\ 18}^4)}{32} = \frac{9.680 \cdot 10^{-5} \text{ kg m}^2}{32}, \quad (36)$$

$$I_{z_{17}} = \frac{\rho \cdot \pi \cdot R^2 \cdot B_{17} \cdot (D_{out\ med\ 17}^4 - D_{inn\ 17}^4)}{32} = \frac{1.683 \cdot 10^{-5} \text{ kg m}^2}{32}, \quad (37)$$

$$I_{A8} = \frac{\rho \cdot \pi \cdot D_{m8}^4 \cdot h_8}{32} = 16.574 \cdot 10^{-6} \text{ kg m}^2, \quad (38)$$

$$I_{z_{16}} = \frac{\rho \cdot \pi \cdot R^2 \cdot B_{16} \cdot (D_{out\ med\ 16}^4 - D_{inn\ 16}^4)}{32} = \frac{85.781 \cdot 10^{-5} \text{ kg m}^2}{32}, \quad (39)$$

$$I_{z_{14}} = \frac{\rho \cdot \pi \cdot R^2 \cdot B_{14} \cdot (D_{out\ med\ 14}^4 - D_{inn\ 14}^4)}{32} = \frac{1.201 \cdot 10^{-6} \text{ kg m}^2}{32}, \quad (40)$$

$$I_{A6} = \frac{\rho \cdot \pi \cdot D_{m6}^4 \cdot h_6}{32} = 1.213 \cdot 10^{-6} \text{ kg m}^2, \quad (41)$$

$$I_{z_{12}} = \frac{\rho \cdot \pi \cdot R^2 \cdot B_{12} \cdot (D_{out\ med\ 12}^4 - D_{inn\ 12}^4)}{32} = \frac{2.495 \cdot 10^{-5} \text{ kg m}^2}{32}, \quad (42)$$

$$I_{z_{10}} = \frac{\rho \cdot \pi \cdot R^2 \cdot B_{10} \cdot (D_{out\ med\ 10}^4 - D_{inn\ 10}^4)}{32} = \frac{2.495 \cdot 10^{-5} \text{ kg m}^2}{32}, \quad (43)$$

$$I_{A2} = \frac{\rho \cdot \pi \cdot D_{m2}^4 \cdot h_2}{32} = 0.017 \text{ kg m}^2, \quad (44)$$

$$I_{z_4} = \frac{\rho \cdot \pi \cdot R^2 \cdot (D_{out\ med\ 4}^4 - D_{inn\ 4}^4)}{32} = \frac{3.481 \cdot 10^{-5} \text{ kg m}^2}{32}, \quad (45)$$

$$I_{z_3} = \frac{\rho \cdot \pi \cdot R^2 \cdot B_3 \cdot (D_{out\ med\ 3}^4 - D_{inn\ 3}^4)}{32} = \frac{1.517 \cdot 10^{-6} \text{ kg m}^2}{32}, \quad (46)$$

At this stage, the reduced total reflected inertia on the shaft drive motor of the IR 6 axis could be evaluated as follows:

$$J_{MOT+BRAKE} = J_{MOT} + J_{BRAKE} = (0.57 + 0.05) \text{ kg} \cdot \text{cm}^2 = 0.62 \cdot 10^{-4} \text{ kg m}^2, \quad (47)$$

$$J_{RED}^{EM \text{ shaft}} = \left\{ \left[ (J_{RED} J_{MOT} + J_{A7} + J_{Z18}) \cdot \left(\frac{z_{17}}{z_{18}}\right)^2 + J_{Z17} + J_{A8} + J_{Z16} \right] \cdot \left(\frac{z_{14}}{z_{15}}\right)^2 + J_{Z14} + J_{A6} + J_{Z12} \right] \cdot \left(\frac{z_{10}}{z_{12}}\right)^2 + J_{Z10} + J_{A2} + J_{Z4} \right\} \cdot \left(\frac{z_2}{z_4}\right)^2 + J_{Z2} + J_{MOT+BRAKE} = 0.0043926 + J_{MOT+BRAKE} \text{ [kg m}^2\text{]}. \quad (48)$$

Similar calculus has been performed for identifying specific loads applied to driving motors of axis 5 and 4, taking into account their specific mechanical structure and involved appropriate components reflected inertia [3, 10].

#### 4.5. Applying the optimum sizing and selection criteria for IR driving motors

Having to our disposal all above calculus results, the iterative procedure optimum sizing and selection criteria for IR driving motors may be started [3]. For this purpose, the kinematic criteria, the static criteria, the dynamic criteria, and the performance parameters criteria applying will be continued to be applied up to their complete accomplishing by a specific range and size of the available servomotors [14].

However, to perform the iterative calculation algorithm for optimum sizing and selection of the driving motors, from all ranges of available servomotors, considering that all specific mechanical components

involve speed reducing ratio, first of all, from the same servomotor series, will be selected the servomotors ranges having the maximum available rated speed. In the meantime, because ideally is that the servomotors have the lower available size the selection procedure will start by checking the 9C1 series of servomotors and will continue with 9C4 and respectively 9C5 series. Thus, first considered servomotor (marked in red in Fig. 27), will have the rated speed of 6,000 rot/min (9C1.1.60...M). After checking of all servomotors from this half-range series, the next half-range series to be tested will be the one having the rated speed of 3,000 rot/min (9C1.1.30...M) having the same size as previously tested servomotors but lower rated speed. The procedure will continue by testing of the half-range series of servomotors having the rated speed of 4,000 rot/min (9C4.1.40...M) and successively the half-range series of servomotors having the rated speed of 3,000 rot / min (9C4.1.30...M). The last to be tested will be the half-range series 9C5.2.30...M and last of all the half-range series 9C5.2.2.30...M servomotors.

In order to take into account the specific mechanical and functional characteristics of the motor brakes, additional information must be taken into account.

Following all above-mentioned consideration, the calculus algorithm performed for successive checking the motor size versions available from the mentioned series is presented for the kinematic criteria, the static criteria, the dynamic criteria and the performance parameters criteria [3, 10].

9C series technical details														
Type	Continuous torque at zero speed <sup>1)</sup>	Current at continuous torque <sup>1) 2)</sup>	Rated torque <sup>3)</sup>	Rated current <sup>3) 4)</sup>	Rated speed	Rated frequency	Mechanical rated power <sup>5)</sup>	Peak torque	Current at peak torque <sup>1) 3)</sup>	Torque constant <sup>1) 3)</sup>	B.e.m.f. between phases at rated speed <sup>1) 2) 3)</sup>	Moment of inertia of rotor <sup>6)</sup>	Moment of inertia of rotor + brake <sup>6)</sup>	Weight <sup>7) 8)</sup>
	$T_{0n}$ [Nm]	$I_{cn}$ [A]	$T_{rn}$ [Nm]	$I_{rn}$ [A]	$n_{rn}$ [r/min]	$f_{rn}$ [Hz]	$P_{rn}$ [kW]	$T_{pn}$ [Nm]	$I_{pn}$ [A]	$K_t$ [Nm/A]	$V$ [V]	$J_r$ [kgcm <sup>2</sup> ]	$J_{r+b}$ [kgcm <sup>2</sup> ]	$W$ [kg]
9C1.1.30...M	1.4	1.3	1.3	1.4	3000	250.0	0.41	4.1	4.5	1.147	208	0.57	0.62	3.0
9C1.2.30...M	2.3	1.8	2	1.7	3000	250.0	0.63	6.9	6.1	1.440	261	1.04	1.09	4.0
9C1.3.30...M	3.2	2.7	2.8	2.5	3000	250.0	0.88	9.6	9.0	1.350	245	1.51	1.56	5.0
9C1.4.30...M	4.2	3.3	3.5	2.9	3000	250.0	1.10	12.6	11.1	1.440	261	1.99	2.04	6.0
9C1.1.60...M	1.4	2.1	1.2	2.0	6000	500.0	0.75	4.1	7.1	0.720	261	0.57	0.62	3.0
9C1.2.60...M	2.3	3.6	1.6	2.7	6000	500.0	1.01	6.9	12.1	0.720	261	1.04	1.09	4.0
9C1.3.60...M	3.2	5.2	2.3	3.9	6000	500.0	1.45	9.6	17.3	0.702	255	1.51	1.56	5.0
9C1.4.60...M	4.2	6.5	2.5	4.1	6000	500.0	1.57	12.6	21.6	0.738	268	1.99	2.04	6.0
9C4.1.30...M	4.3	3.0	3.9	2.8	3000	250.0	1.23	12.9	9.8	1.654	300	4.0	4.7	5.6
9C4.2.30...M	7.5	5.0	6.1	4.3	3000	250.0	1.92	22.5	16.7	1.704	309	7.6	8.3	7.9
9C4.3.30...M	9.4	6.0	6.9	4.6	3000	250.0	2.17	28.2	19.9	1.786	324	11.1	11.8	10.2
9C4.4.30...M	12.0	8.2	7.5	5.4	3000	250.0	2.36	36.0	27.3	1.665	302	14.7	15.4	12.5
9C4.1.40...M	4.3	4.0	3.7	3.6	4000	333.3	1.55	12.9	13.2	1.232	298	4.0	4.7	5.6
9C4.2.40...M	7.5	6.9	5.4	5.2	4000	333.3	2.26	22.5	23.1	1.232	298	7.6	8.3	7.9
9C4.3.40...M	9.4	7.8	5.8	5.1	4000	333.3	2.43	28.2	26.1	1.365	330	11.1	11.8	10.2
9C4.4.40...M	12.0	10.0	6.3	5.5	4000	333.3	2.64	36.0	33.3	1.365	330	14.7	15.4	12.5
9C5.2.20...M	12.3	6.1	10.3	5.3	2000	166.7	2.16	36.9	20.2	2.307	279.0	21.8	23.6	15.5
9C5.3.20...M	18.4	9.2	14.8	7.8	2000	166.7	3.10	55.2	30.7	2.272	274.7	31.6	33.4	19.2
9C5.4.20...M	23.5	11.9	17.1	9.1	2000	166.7	3.58	70.5	39.6	2.249	272.0	41.4	43.2	22.9
9C5.5.20...M	26.0	12.0	20.0	9.8	2000	166.7	4.19	78.0	40.2	2.452	296.5	51.2	53.0	26.6
9C5.6.20...M	30.0	13.1	22.0	10.1	2000	166.7	4.61	90.0	43.8	2.596	313.9	61.0	62.8	30.3
9C5.2.30...M	12.3	9.2	9.0	7.1	3000	250.0	2.83	36.9	30.8	1.515	274.7	21.8	23.6	15.5
9C5.3.30...M	18.4	12.4	12.4	8.9	3000	250.0	3.90	55.2	41.3	1.688	306.1	31.6	33.4	19.2
9C5.4.30...M	23.5	15.4	14.0	9.7	3000	250.0	4.40	70.5	51.4	1.731	313.9	41.4	43.2	22.9
9C5.5.30...M	26.0	17.1	17.0	11.8	3000	250.0	5.34	78.0	56.9	1.731	313.9	51.2	53.0	26.6
9C5.6.30...M	30.0	19.7	18.0	12.4	3000	250.0	5.85	90.0	65.7	1.731	313.9	61.0	62.8	30.3

Optional holding brake specification								
Motor type	Rated voltage	Input power	Input current	Braking torque	Armature release time	Armature pull-in time	Inertia	Additional weight with brake
	[VDC]	[W]	[A]	[Nm]	[ms]	[ms]	[kgcm <sup>2</sup> ]	[kg]
9C1	24	6.3	0.26	2.5	30	50	0.102	0.6
9C4	24	19.5	0.81	16	30	70	0.73	1.5
9C5	24	28.0	1.17	30	30	75	1.82	2.2

Fig. 27. Constructive and functional characteristics of ABB 9C servomotors series [14].

## 4.5.1. The kinematic criteria

$$n_{\max nec EM} \leq n_{\max EM shaft} \quad (49)$$

$$n_{joint 6} = 83.26 \text{ rot/min.} \quad (50)$$

$$n_{\max nec EM} = \frac{n_{joint 6}}{\frac{z_1}{z_2} \cdot \frac{z_3}{z_4} \cdot \frac{z_5}{z_6} \cdot \frac{z_7}{z_8}} = \frac{83.26}{\frac{1}{2} \cdot \frac{1}{5} \cdot \frac{1}{2}} = 1665.2 \text{ rot/min,} \quad (51)$$

$$9C1.1.60 \Rightarrow n_{\max nec EM} = 1665.2 \text{ rot/min} < n_{\max EM shaft} = 6000 \frac{rot}{min} \quad (52)$$

$$9C1.2.60 \Rightarrow n_{\max nec EM} = 1665.2 \text{ rot/min} < n_{\max EM shaft} = 6000 \text{ rot/min} \quad (53)$$

$$9C1.3.60 \Rightarrow n_{\max nec EM} = 1665.2 \text{ rot/min} < n_{\max EM shaft} = 6000 \text{ rot/min} \quad (54)$$

$$9C1.4.60 \Rightarrow n_{\max nec EM} = 1665.2 \text{ rot/min} < n_{\max EM shaft} = 6000 \text{ rot/min} \quad (55)$$

As above illustrated, all the servomotors of series 9C1.\*.60 are satisfying the specific restrictions of the kinematic criteria.

## 4.5.2. The static criteria

$$M_{st red}^{EM shaft} \leq M_{rated torque}^{EM shaft} \quad (56)$$

$$P_{st-sch-radial joint 6} = 0.6 \cdot F_R + 0.5 \cdot F_A = 0.6 \cdot 215.57 - 0.5 \cdot 180.88 = 38.902 \text{ N} \quad (57)$$

$$d_{m bearing joint 6} = \frac{d+D}{2} = \frac{37+43}{2} = 40 \text{ mm,} \quad (58)$$

$$M_{friction joint 6} = f_{preload} \cdot P_{st-sch-radial} \cdot \frac{d_{mod}}{2} = 1.3 \cdot 38.902 \cdot \frac{25 \cdot 10^{-3}}{2} = 0.6322 \text{ Nm} \quad (59)$$

$$M_{st joint 6} = M_{friction pret bear} = 0.6322 \cdot \text{Nm,} \quad (60)$$

$$M_{st red}^{EM shaft} = M_{st joint 6} \cdot \frac{z_1}{z_2} \cdot \frac{z_3}{z_4} \cdot \frac{z_5}{z_6} \cdot \frac{z_7}{z_8} = 0.6322 \cdot \frac{1}{2} \cdot \frac{1}{5} \cdot \frac{1}{2} = 0.0316 \text{ Nm} \quad (61)$$

$$9C1.1.60 \Rightarrow M_{st red}^{EM shaft} = 0.0316 \text{ Nm} \leq M_{rated torque}^{EM shaft} = 1.2 \text{ Nm} \quad (62)$$

$$9C1.2.60 \Rightarrow M_{st red}^{EM shaft} = 0.0316 \text{ Nm} \leq M_{rated torque}^{EM shaft} = 1.6 \text{ Nm} \quad (63)$$

$$9C1.3.60 \Rightarrow M_{st red}^{EM shaft} = 0.0316 \text{ Nm} \leq M_{rated torque}^{EM shaft} = 2.3 \text{ Nm} \quad (64)$$

$$9C1.4.60 \Rightarrow M_{st red}^{EM shaft} = 0.0316 \text{ Nm} \leq M_{rated torque}^{EM shaft} = 2.5 \text{ Nm} \quad (65)$$

As above illustrated all the servomotors of series 9C1.4.60 are satisfying too the specific restrictions of the static criteria.

## 4.5.3. The dynamic criteria

$$M_{dintot} = M_{st red}^{EM shaft} + M_{inertial}^{EM shaft} \quad (66)$$

$$M_{dntot} \leq M_{peak torque}^{EM shaft} \quad (67)$$

$$M_{st joint 6} = M_{friction bearing} = 0.6322 \text{ Nm.} \quad (68)$$

$$M_{st red}^{EM shaft} = M_{st joint 6} \cdot \frac{z_1}{z_2} \cdot \frac{z_3}{z_4} \cdot \frac{z_5}{z_6} \cdot \frac{z_7}{z_8} = 0.6322 \cdot \frac{1}{2} \cdot \frac{1}{5} \cdot \frac{1}{2} = 0.0316 \text{ Nm,} \quad (69)$$

$$M_{inertial}^{EM shaft} = J_{RED}^{EM shaft} \cdot \varepsilon_{EM shaft} \quad (70)$$

$$9C1.1.60 \Rightarrow J_{MOT+BRAKE} = 0.62 \cdot 10^{-2} \text{ kg m}^2, \quad (71)$$

$$9C1.2.60 \Rightarrow J_{MOT+BRAKE} = 1.09 \cdot 10^{-2} \text{ kg m}^2, \quad (72)$$

$$9C1.3.60 \Rightarrow J_{MOT+BRAKE} = 1.56 \cdot 10^{-2} \text{ kg m}^2, \quad (73)$$

$$9C1.4.60 \Rightarrow J_{MOT+BRAKE} = 2.04 \cdot 10^{-2} \text{ kg m}^2. \quad (74)$$

In order to evaluate the second term of the dynamic torque specific calculation for the reflected inertia need to be performed by taking into account the different characteristics of each size of servomotors and appropriate associated brake.

## 9C1.1.60

$$J_{RED}^{EM shaft} = \left\{ \left[ \left( J_{RED joint 6} + J_{A7} + J_{Z18} \right) \cdot \left( \frac{z_{17}}{z_{18}} \right)^2 + J_{Z17} + J_{A8} + J_{Z16} \right] \cdot \left( \frac{z_{14}}{z_{16}} \right)^2 + J_{Z14} + J_{A9} + J_{Z12} \right\} \cdot \left( \frac{z_{10}}{z_{12}} \right)^2 + J_{Z10} + J_{A2} + J_{Z8} \right\} \cdot \left( \frac{z_3}{z_4} \right)^2 + J_{Z6} + J_{MOT+BRAKE} = 0.01059 \text{ kg m}^2 \quad (75)$$

## 9C1.2.60

$$J_{RED}^{EM shaft} = \left\{ \left[ \left( J_{RED joint 6} + J_{A7} + J_{Z18} \right) \cdot \left( \frac{z_{17}}{z_{18}} \right)^2 + J_{Z17} + J_{A8} + J_{Z16} \right] \cdot \left( \frac{z_{14}}{z_{16}} \right)^2 + J_{Z14} + J_{A9} + J_{Z12} \right\} \cdot \left( \frac{z_{10}}{z_{12}} \right)^2 + J_{Z10} + J_{A2} + J_{Z8} \right\} \cdot \left( \frac{z_3}{z_4} \right)^2 + J_{Z6} + J_{MOT+BRAKE} = 0.01529 \text{ kg m}^2 \quad (76)$$

## 9C1.3.60

$$J_{RED}^{EM shaft} = \left\{ \left[ \left( J_{RED joint 6} + J_{A7} + J_{Z18} \right) \cdot \left( \frac{z_{17}}{z_{18}} \right)^2 + J_{Z17} + J_{A8} + J_{Z16} \right] \cdot \left( \frac{z_{14}}{z_{16}} \right)^2 + J_{Z14} + J_{A9} + J_{Z12} \right\} \cdot \left( \frac{z_{10}}{z_{12}} \right)^2 + J_{Z10} + J_{A2} + J_{Z8} \right\} \cdot \left( \frac{z_3}{z_4} \right)^2 + J_{Z6} + J_{MOT+BRAKE} = 0.01992 \text{ kg m}^2 \quad (77)$$

## 9C1.4.60

$$J_{RED}^{EM shaft} = \left\{ \left[ \left( J_{RED joint 6} + J_{A7} + J_{Z18} \right) \cdot \left( \frac{z_{17}}{z_{18}} \right)^2 + J_{Z17} + J_{A8} + J_{Z16} \right] \cdot \left( \frac{z_{14}}{z_{16}} \right)^2 + J_{Z14} + J_{A9} + J_{Z12} \right\} \cdot \left( \frac{z_{10}}{z_{12}} \right)^2 + J_{Z10} + J_{A2} + J_{Z8} \right\} \cdot \left( \frac{z_3}{z_4} \right)^2 + J_{Z6} + J_{MOT+BRAKE} = 0.02479 \text{ kg m}^2 \quad (78)$$

$$\varepsilon_{EM shaft} = \frac{\varepsilon_{joint 6}}{\frac{z_1}{z_2} \cdot \frac{z_3}{z_4} \cdot \frac{z_5}{z_6} \cdot \frac{z_7}{z_8}} = \frac{17.44}{\frac{1}{2} \cdot \frac{1}{5} \cdot \frac{1}{2}} = 348.8 \text{ rad/s}^2, \quad (79)$$

$$M_{inertial}^{EM\ shaft} = J_{RED}^{EM\ shaft} \cdot \varepsilon_{EM\ shaft}, \quad (80)$$

$$9C1.1.60 \Rightarrow M_{inertial}^{EM\ shaft} = 0.01059 \cdot 348.8 = 3.69379 \text{ Nm}, \quad (81)$$

$$9C1.2.60 \Rightarrow M_{inertial}^{EM\ shaft} = 0.01529 \cdot 348.8 = 5.33315 \text{ Nm}, \quad (82)$$

$$9C1.3.60 \Rightarrow M_{inertial}^{EM\ shaft} = 0.01992 \cdot 348.8 = 6.94809 \text{ Nm}, \quad (83)$$

$$9C1.4.60 \Rightarrow M_{inertial}^{EM\ shaft} = 0.02479 \cdot 348.8 = 8.64675 \text{ Nm}, \quad (84)$$

$$M_{din\ tot} = M_{st\ red}^{EM\ shaft} + M_{inertial}^{EM\ shaft} \leq M_{peak\ torque}^{EM\ shaft}, \quad (85)$$

$$9C1.1.60 \Rightarrow M_{din\ tot} = M_{st\ red}^{EM\ shaft} + M_{inertial}^{EM\ shaft} = 0.0316 + 3.69379 = 3.72539 \text{ Nm}, \quad (86)$$

$$9C1.2.60 \Rightarrow M_{din\ tot} = M_{st\ red}^{EM\ shaft} + M_{inertial}^{EM\ shaft} = 0.0316 + 5.33315 = 5.36475 \text{ Nm}, \quad (87)$$

$$9C1.3.60 \Rightarrow M_{din\ tot} = M_{st\ red}^{EM\ shaft} + M_{inertial}^{EM\ shaft} = 0.0316 + 6.94809 = 6.97969 \text{ Nm}, \quad (88)$$

$$9C1.4.60 \Rightarrow M_{din\ tot} = M_{st\ red}^{EM\ shaft} + M_{inertial}^{EM\ shaft} = 0.0316 + 8.64675 = 8.67835 \text{ Nm}, \quad (89)$$

$$9C1.1.60 \Rightarrow M_{din\ tot} = 3.72539 \text{ Nm} < M_{peak\ torque}^{EM\ shaft} = 4.1 \text{ Nm}, \quad (90)$$

$$9C1.2.60 \Rightarrow M_{din\ tot} = 5.36475 \text{ Nm} < M_{peak\ torque}^{EM\ shaft} = 6.9 \text{ Nm}, \quad (91)$$

$$9C1.3.60 \Rightarrow M_{din\ tot} = 6.97969 \text{ Nm} < M_{peak\ torque}^{EM\ shaft} = 9.6 \text{ Nm}, \quad (92)$$

$$9C1.4.60 \Rightarrow M_{din\ tot} = 8.67835 \text{ Nm} < M_{peak\ torque}^{EM\ shaft} = 12.6 \text{ Nm}. \quad (93)$$

As above illustrated all the servomotors of series 9C1.4.60 are satisfying too the specific restrictions of the dynamic criteria.

#### 4.5.4. The performance parameter criteria

$$t_{acc} = \frac{4}{375} \cdot J_{RED}^{EM\ shaft} \cdot n_{max\ EM\ shaft} \cdot \left( \frac{0.3}{M_{peak\ torque}^{EM\ shaft} - M_{st\ red}^{EM\ shaft}} + \frac{0.7}{\frac{1}{5} M_{peak\ torque}^{EM\ shaft} - M_{st\ red}^{EM\ shaft}} \right) \leq 0.35 \text{ s}, \quad (94)$$

$$t_{break} = \frac{4}{375} \cdot J_{RED}^{EM\ shaft} \cdot \frac{n_{max\ EM\ shaft}}{M_{EM\ breaking}^{EM\ shaft} - M_{st\ red}^{EM\ shaft}} \leq 0.35 \text{ s}, \quad (95)$$

$$9C1.1.60 \Rightarrow J_{MOT+BRAKE} = 0.62 \cdot 10^{-2} \text{ kg m}^2, \quad J_{RED}^{EM\ shaft} = 0.0105926 \text{ kg m}^2, \quad (96)$$

$$9C1.2.60 \Rightarrow J_{MOT+BRAKE} = 1.09 \cdot 10^{-2} \text{ kg m}^2, \quad J_{RED}^{EM\ shaft} = 0.0152926 \text{ kg m}^2, \quad (97)$$

$$9C1.3.60 \Rightarrow J_{MOT+BRAKE} = 1.56 \cdot 10^{-2} \text{ kg m}^2, \quad J_{RED}^{EM\ shaft} = 0.0199926 \text{ kg m}^2, \quad (98)$$

$$9C1.4.60 \Rightarrow J_{MOT+BRAKE} = 2.04 \cdot 10^{-2} \text{ kg m}^2, \quad J_{RED}^{EM\ shaft} = 0.0247926 \text{ kg m}^2. \quad (99)$$

$$9C1.1.60 - 6000 \text{ rot / min} \\ t_{acc} = \frac{4}{375} \cdot 0.0105926 \cdot 6000 \cdot \left( \frac{0.3}{4.1 - 0.0316} + \frac{0.7}{\frac{1}{5} \cdot 4.1 - 0.0316} \right) = 0.651 \text{ sec} > 0.35 \text{ sec}, \quad (100)$$

$$t_{break} = \frac{4}{375} \cdot 0.0105926 \cdot \frac{6000}{2.5 - 0.0316} = 0.275 \text{ sec} \leq 0.35 \text{ sec}, \quad (101)$$

$$9C1.2.60 - 6000 \text{ rot/min} \\ t_{acc} = \frac{4}{375} \cdot 0.0152926 \cdot 6000 \cdot \left( \frac{0.3}{6.9 - 0.0316} + \frac{0.7}{\frac{1}{5} \cdot 6.9 - 0.0316} \right) = 0.147 \leq 0.35 \text{ sec}, \quad (102)$$

$$t_{break} = \frac{4}{375} \cdot 0.0152926 \cdot \frac{6000}{2.5 - 0.0316} = 0.396 \text{ sec} > 0.35 \text{ sec}, \quad (103)$$

$$9C1.3.60 - 6000 \text{ rot / min} \\ t_{acc} = \frac{4}{375} \cdot 0.0199926 \cdot 6000 \cdot \left( \frac{0.3}{9.6 - 0.0316} + \frac{0.7}{\frac{1}{5} \cdot 9.6 - 0.0316} \right) = 0.515 \text{ sec} > 0.35 \text{ sec}, \quad (104)$$

$$t_{break} = \frac{4}{375} \cdot 0.0199926 \cdot \frac{3000}{2.5 - 0.0316} = 0.519 \text{ sec} > 0.35 \text{ sec}, \quad (105)$$

$$9C1.4.60 - 6000 \text{ rot / min} \\ t_{acc} = \frac{4}{375} \cdot 0.0247926 \cdot 6000 \cdot \left( \frac{0.3}{12.6 - 0.0316} + \frac{0.7}{\frac{1}{5} \cdot 12.6 - 0.0316} \right) = 0.484 \text{ sec} > 0.35 \text{ sec}, \quad (106)$$

$$t_{break} = \frac{4}{375} \cdot 0.0247926 \cdot \frac{6000}{2.5 - 0.0316} = 0.642 \text{ sec} > 0.35 \text{ sec}. \quad (107)$$

As can be seen, no servomotor from series 9C1.\*.60...M (having the rated speed of 6,000 rot/min) does not meet the performance parameter criteria, so next series of servomotors (9C1.\*.30...M, having the same size but lower rated speed) will be tested only for this criterion:

$$9C1.1.30 - 3000 \text{ rot/min} \\ t_{acc} = \frac{4}{375} \cdot 0.0105926 \cdot 3000 \cdot \left( \frac{0.3}{4.1 - 0.0316} + \frac{0.7}{\frac{1}{5} \cdot 4.1 - 0.0316} \right) = 0.326 \text{ sec} < 0.35 \text{ sec}, \quad (108)$$

$$t_{break} = \frac{4}{375} \cdot 0.0105926 \cdot \frac{3000}{2.5 - 0.0316} = 0.138 \text{ sec} \leq 0.35 \text{ sec}. \quad (109)$$

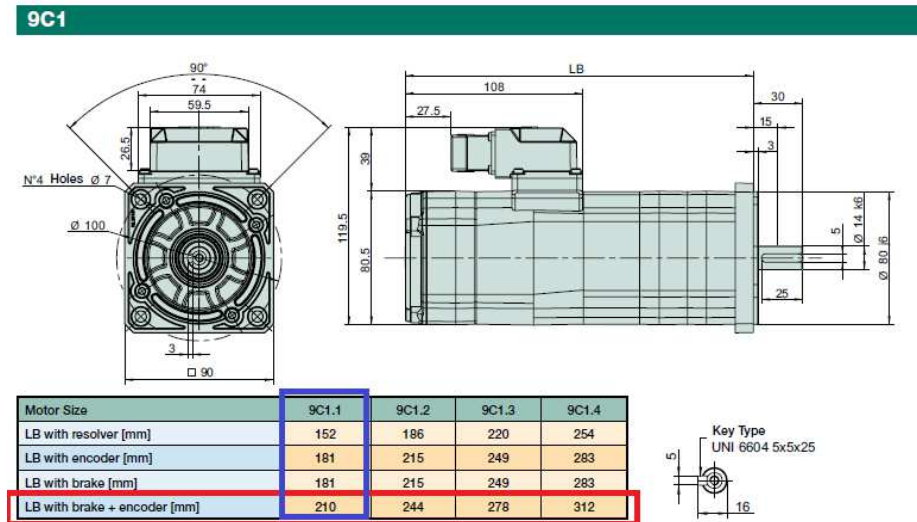


Fig. 28. Final selected servomotor dimensional characteristics.

As the first dimension of the servomotor in this series with half range, it respects both restrictions imposed by the performance parameters, the final optimum selected driving motor for axis 6 will be the servomotor model 9C1.1.30 (having a 3,000 rot/min rated speed).

Final selected servomotor dimensional characteristics are presented in Fig. 28.

## 5. CONCLUSIONS

In developing new robotic cells two approaches may be of interest presently: to use a pre-engineered robotic cell and respectively to develop a custom designed robotic cell for arc welding. Discussion on issues regarding the involved advantages and disadvantages of each approach and conclusions are presented in the first part of the paper, as well as an improved model of a custom designed arc welding robotic cell.

Second part of the paper deals about a specific calculus algorithm developed for optimum motor selection of the industrial robots. Specific steps of calculation procedure detailed in the paper may be already used for a large number of industrial robot models whatever they are used for arc welding purpose or another industrial application. The application of the calculus procedure is exemplified in the paper regarding the optimum selection of the driving motors for the last three NC axis of an ABB IRB 2400 articulated arm industrial robot, but however the algorithm may be extended for the sizing and optimum selection of all IR driving motors.

In the meantime, the calculus algorithm may be also used for same purpose for other IR models having similar design of the end-effector orienting sub-system.

The proposed algorithm has been intensively tested for many industrial robot models and the results of calculation were validated for all IR analyzed models.

## REFERENCES

- [1] M. Guerry, C. Muller, W. Kraus, S. Bieller, *World Robotics 2021*, International Federation of Robotics, Frankfurt am Main, Germany, 2021.

- [2] A.F. Nicolescu, D.A. Marinescu, M. Ivan, G.C. Avram, *Concepția și exploatarea sistemelor de producție robotizate* (Design and operation of robotic production systems), Edit. Politehnica Press, Bucharest, 2011.
- [3] A.F. Nicolescu, *Concepția și exploatarea roboților industriali – Metodologii de calcul pentru proiectarea și verificarea condițiilor de exploatare a roboților industriali* (Design and operation of industrial robots – Calculation methodologies for designing and verifying the operating conditions of industrial robots), Edit. Politehnica Press, Bucharest, 2020.
- [4] *FlexArc® – Robotic Arc-Welding Cells Modular solutions to meet your requirements*, available at: <https://library.e.abb.com>, accessed 2021-10-10.
- [5] *The Definitive Guide to Automation for Welding and Metal Fabrication*, available at: <https://www.lincolnelectric.com/en/Products/Automation/Robotic-Welding>, accessed 2021-10-10.
- [6] *Robot Welding System Standard Cells*, available at: [https://www.robotolution.de/standard\\_cells\\_en](https://www.robotolution.de/standard_cells_en), accessed 2021-10-10.
- [7] *Welding Lines and Systems Efficient, process-reliable, fully synchronized*, available at: <https://www.yaskawa.eu.com/catalogs>, accessed 2021-10-10.
- [8] *Cell strategy* available at: <https://robotsoneright.com/Articles>, accessed 2021-10-10.
- [9] Mark Miller, *Robotic Welding System Design: A Need-to-Know Guide for Automated Welding*, available at: <https://www.forcedesign.biz/blog/robotic-welding-system-design-automated-welding> [10]
- [10] C. Dumitrașcu, *Arc welding robotic cell*, graduation project, Politehnica University of Bucharest, 2019.
- [11] *VirtualArc*, available at: <https://new.abb.com/products/robotics/application-software/>, accessed 2021-10-10.
- [12] *RoboDK programming and simulation software*, available at: <https://robodk.com/>, accessed 2021-10-10.
- [13] *ABB IRB 2400 Product specification*, available at: <https://library.e.abb.com>, accessed 2021-10-10.
- [14] *ABB servo motors 9C series for ABB high performance machinery drives*, available at: <https://search.abb.com/library/>, accessed 2021-10-10.